

# Highly Oriented Gold Nanoribbons by the Reduction of Aqueous Chloroaurate Ions by Hexadecylaniline Langmuir Monolayers

Anita Swami, Ashavani Kumar, PR. Selvakannan, Saikat Mandal, Renu Pasricha, and Murali Sastry\*

Materials Chemistry Division, National Chemical Laboratory, Pune 411 008, India

Received September 13, 2002

Revised Manuscript Received November 11, 2002

It is now recognized that, in addition to nanoparticle size and composition, nanoparticle shape plays an important role in modulating its electronic and chemical properties.<sup>1–4</sup> Million-fold fluorescence enhancement in gold nanorods<sup>1</sup> and the first observation of distinct quadrupole plasmon resonances in silver nanoprisms<sup>2</sup> are some of the exciting shape-dependent properties reported recently. Insofar as noble metal nanoparticles such as silver and gold are concerned, a plethora of solution-based experimental procedures have been developed for shape modulation.<sup>1,2,5–12</sup> While most of the protocols result in predominantly rodlike nanoparticles of tunable aspect ratios<sup>1,7–10</sup> and nanofibers,<sup>5–7,12</sup> growth of other morphologies such as triangular<sup>2,7,11</sup> and flat hexagonal particles<sup>11</sup> have been observed less frequently.

Shape anisotropy in gold nanoparticles has also been introduced by synthesizing them in constrained environments<sup>13</sup> or at suitable interfaces such as those provided by Langmuir monolayers.<sup>14</sup> Surprisingly, the use of the air–water interface for achieving nanoparticle shape control remains largely unexplored and underexploited. We have recently demonstrated a simple one-step process for the synthesis of hydrophobic spherical gold nanoparticles using the multifunctional molecule 4-hexadecylaniline (HDA) that electrostatically complexes with aqueous chloroaurate ions, reduces them,

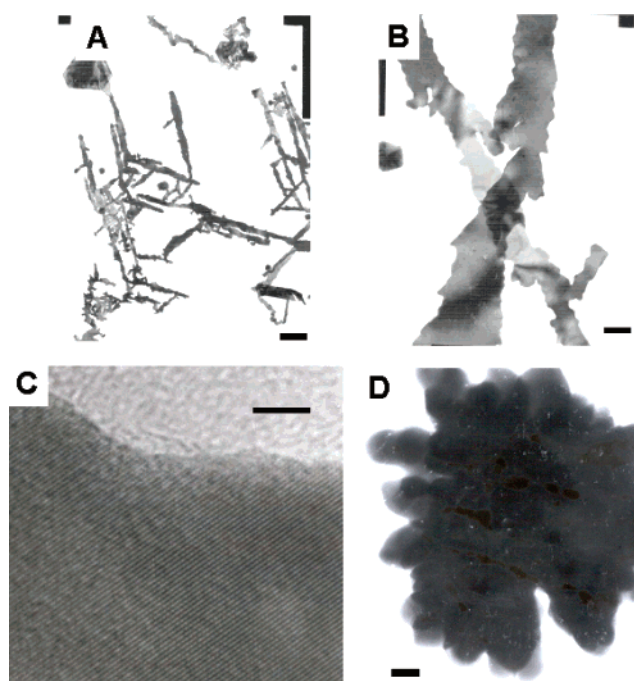


**Figure 1.** (A–C) TEM pictures at different magnifications of gold nanoribbons grown under an HDA monolayer. Scale bars: A, 200 nm; B, 50 nm; C, 5 nm. (D) TEM image of a nanogold aggregate by hydrazine reduction of  $\text{AuCl}_4^-$  ions complexed with HDA monolayer; scale bar = 50 nm.

and caps the nanoparticles thus formed.<sup>15</sup> In this communication, we demonstrate that the spontaneous reduction of chloroaurate ions present in the subphase by Langmuir monolayers of HDA leads to the formation of highly oriented, flat gold sheets and ribbonlike nanocrystals bound to the monolayer. This one-step process constrains growth of the gold nanocrystals to within the plane of the Langmuir monolayer and sets it apart from existing air–water interface wet-chemistry methods where the role of the Langmuir monolayer is passive and the growth zone is much more delocalized.<sup>14</sup>

Transmission electron microscopy (TEM) images recorded from a two-monolayer (ML) Langmuir–Blodgett (LB) film of gold nanoparticles prepared by the reduction of chloroaurate ions in the subphase by the HDA Langmuir monolayer for 36 h<sup>16</sup> revealed the presence of a very large concentration of flat gold nanoribbons and, occasionally, triangular gold particles (Figure 1A). A higher magnification image of two gold nanoribbons crossing one another is shown in Figure 1B. While an

\* To whom correspondence should be addressed. E-mail: sastry@ems.ncl.res.in.

- (1) El-Sayed, M. *Acc. Chem. Res.* **2001**, *34*, 257.
- (2) Jin, R.; Cao, Y.-W.; Mirkin, C. A.; Kelly, K. L.; Schatz, G. C.; Zheng, J. G. *Science* **2001**, *294*, 1901.
- (3) Peng, X.; Manna, L.; Yang, W.; Wickham, J.; Scher, E.; Kadavavich, A.; Alivisatos, A. P. *Nature* **2000**, *404*, 59.
- (4) Pinna, N.; Weiss, K.; Urban, J.; Pileni, M.-P. *Adv. Mater.* **2001**, *13*, 261.
- (5) Esumi, K.; Matsuhisa, K.; Torigoe, K. *Langmuir* **1995**, *11*, 3285.
- (6) Kameo, A.; Suzuki, A.; Torigoe, K.; Esumi, K. *J. Colloid Interface Sci.* **2001**, *241*, 289.
- (7) Leontidis, E.; Kleitou, K.; Kyprianidou-Leonidou, T.; Bekiari, V.; Lianos, P. *Langmuir* **2002**, *18*, 3659.
- (8) Brown, K. R.; Walter, D. C.; Natan, M. J. *Chem. Mater.* **2000**, *12*, 306.
- (9) Jana, N. R.; Gearheart, L.; Murphy, C. J. *J. Phys. Chem. B* **2001**, *105*, 4065.
- (10) Zhou, Y.; Wang, C. Y.; Zhu, Y. R.; Chen, Z. Y. *Chem. Mater.* **1999**, *11*, 2310.
- (11) Malikova, N.; Pastoriza-Santos, I.; Scheirhorn, M.; Kotov, N. A.; Liz-Marzan, L. M. *Langmuir* **2002**, *18*, 3694.
- (12) Zhu, Z.; Liu, S.; Palchik, O.; Koltypin, Y.; Gedanken, A. *Langmuir* **2000**, *16*, 6396.
- (13) Pike, J. K.; Byrd, H.; Morrone, A. A.; Talham, D. R. *J. Am. Chem. Soc.* **1993**, *115*, 8497.
- (14) Yi, K. C.; Mendieta, V. S.; Castanares, R. L.; Meldrum, F. C.; Wu, C.; Fendler, J. H. *J. Phys. Chem.* **1995**, *99*, 9869.

- (15) Selvakannan, PR.; Mandal, S.; Pasricha, R.; Adyanthaya, S. D.; Sastry, M. *Chem. Commun.* **2002**, 1334.

(16) The HDA Langmuir monolayer was spread on the surface of a  $10^{-4}$  M  $\text{HAuCl}_4$  solution from chloroform in a 611 Nima Langmuir trough equipped with a Wilhelmy balance for pressure sensing. After measurement of surface pressure–monolayer area ( $\pi$ – $A$ ) isotherms, the HDA monolayer was compressed to a surface pressure of 25 dyn/cm and maintained at this pressure for 36 h in the dark. Thereafter, the gold nanoribbon–HDA complex monolayer was transferred by the LB method at a surface pressure of 25 dyn/cm onto TEM grids and hydrophobized Si (111) wafers and quartz substrates for further analysis. The control experiment was almost identical to that presented above with the only difference being that after quick compression of the monolayer to 25 dyn/cm surface pressure, the monolayer was exposed to vapors of hydrazine for 30 min in a chamber enclosing the trough.

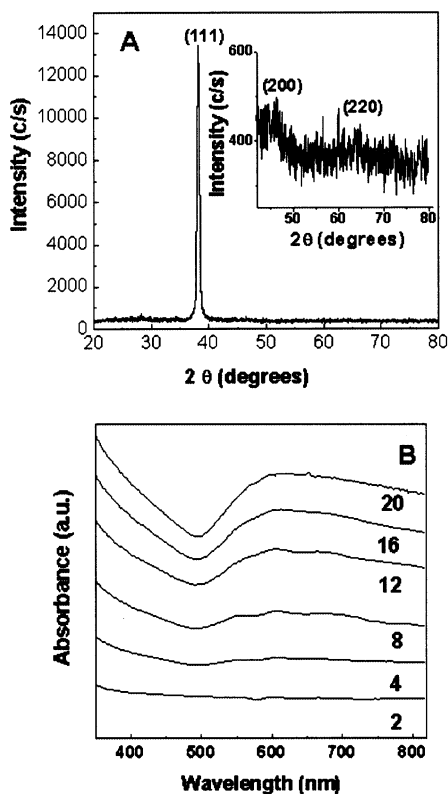


**Figure 2.** (A) XRD pattern recorded from a 20 ML gold nanosheet/-ribbon LB film deposited on glass. The inset shows an expanded region of the XRD pattern highlighting the less intense Bragg reflections. (B) UV-vis spectra recorded from LB films of the gold nanosheet/-ribbons of different thicknesses (indicated next to the respective spectra) deposited on quartz.

estimate of the thickness of the ribbons and sheets in this study could not be made, the contrast in the region of overlap clearly shows that the gold nanostructures are extremely thin. The dark bands observed in the structures are due to strains in the ribbons from buckling during growth or deposition of the LB film. A high-resolution TEM image of an individual gold nanoribbon is shown in Figure 1C. The lattice corresponding to fcc gold is clearly seen in this nanoribbon.

The boundary of the nanoribbons is highly serrated (Figure 1B), suggesting the possibility of self-assembly of smaller triangular units. TEM images were recorded as a function of time of reaction of  $\text{AuCl}_4^-$  ions with the HDA Langmuir monolayer (see Supporting Information, S1). After 2 h of reaction, finely dispersed gold nanoparticles were observed (S1, A) that expanded with time by the growth of secondary gold nuclei at the periphery of existing gold nanostructures (S1, B, 6 h). Eventually, elongated gold nanoribbons were formed at larger reaction times (S1, C and D) by a random nucleation and growth process. Thus, the serrated edges of the gold nanoribbons appear to be due to a templated growth process rather than assembly of smaller subunits.

Formation of gold nanosheets/ribbons at the air-water interface indicates that growth of the nanocrystalline material is highly localized. Gold nanocrystal growth is also highly face-selective as shown in the XRD pattern recorded from a 20 ML LB film of the gold nano-HDA complex deposited on glass (Figure 2A).<sup>16</sup> The XRD pattern shows primarily the (111) Bragg reflection of fcc gold,<sup>17</sup> indicating highly oriented growth

of the nanocrystals at the air-water interface. The inset shows the XRD pattern on an expanded scale. The (200) and (220) Bragg reflections are extremely weak and considerably broadened relative to the (111) reflection. This interesting feature indicates that gold nanocrystals are highly anisotropic in shape. Attempts were made to estimate the thickness of the gold nanoribbons by monitoring the (00 $l$ ) Bragg reflections in the low  $2\theta$  region of the XRD pattern but signals with good signal-to-noise ratio could not be obtained.

A major advantage of organization of nanoparticles at the air-water interface is that multilayer superlattice films of close-packed nanoparticle assemblies may be deposited by the LB method.<sup>16</sup> Figure 2B shows the UV-vis spectra recorded from LB films of the gold nanoribbon-HDA complexes of different thicknesses deposited on quartz substrates. A broad absorption band centered at ca. 610 nm is observed in the films. This absorption band (due to excitation of surface plasmon vibrations in gold nanoparticles) is normally sharp and occurs in the range 510–530 nm for well-dispersed spherical gold nanoparticles in solution.<sup>1</sup> The shift and broadening of the resonance in the LB films indicates considerable aggregation of the particles as well as a high degree of anisotropy in the particle shape, both conclusions borne out by the TEM results. The absorption at 610 nm increases linearly with film thickness, indicating that the gold nanoparticle multilayers grow in a lamellar fashion.

The TEM and XRD results clearly show the spontaneous reduction of  $\text{AuCl}_4^-$  ions and formation of flat, highly oriented gold nanocrystals of ribbonlike morphology at the air-water interface in the presence of HDA Langmuir monolayers. The amine groups of HDA are protonated at the pH of the chloroauric acid subphase (pH 3.5) and immediately after spreading of the HDA monolayer would electrostatically complex with chloroaurate anions in the subphase. This is supported by the large expansion of the HDA monolayer observed via surface pressure-molecular area ( $\pi$ - $A$ ) isotherm measurements recorded 6 h after HDA spreading (Supporting Information, S2). The process of reduction of the gold ions occurs in a spontaneous fashion and in the dark, resulting in formation of gold nanoribbons at the interface. We believe it is this important aspect that distinguishes our method from other air-water interface synthesis protocols wherein reduction of the metal ions is accomplished separately using gaseous reducing agents such as CO, hydrazine, and UV radiation.<sup>14</sup> In the latter case, the reduction of metal ions would occur in a fairly delocalized region of the interface, thus leading to considerable growth of the crystals away from the interface and formation of gold nanoparticles of triangular, isohedral, and decahedral morphologies.<sup>14</sup> In this study, the HDA molecules not only reduce the  $\text{AuCl}_4^-$  ions at an almost ideal two-dimensional surface but also bind strongly to the gold nanoparticles thus formed, further limiting their growth. Strong binding of alkylamine molecules with colloidal gold particles has been observed before<sup>17</sup> and is most likely to be responsible for the preferred (111) orientation of the gold nanocrystals observed in this study. X-ray photoemis-

(17) Leff, D. V.; Brandt, L.; Heath, J. R. *Langmuir* **1996**, *12*, 4723.

sion spectroscopy (XPS) measurements of 2 ML LB films of the gold nano-HDA complexes formed at different times of reaction yielded a nearly constant 2:1 HDA:Au molar ratio after 3 h of reaction (data not shown). This result indicates that oxidation of HDA molecules consequent to reduction of  $\text{AuCl}_4^-$  prevents further entrapment of  $\text{AuCl}_4^-$  ions at the air-water interface. The supply of gold ions feeding nanoribbon formation is thus limited to only a monolayer of gold ions originally bound to the HDA monolayer. Indirectly, this supports the TEM evidence that the gold nanoribbons are extremely thin. That the ribbonlike gold nanoparticle morphology is indeed due to spontaneous reduction of  $\text{AuCl}_4^-$  ions by the HDA Langmuir monolayer may be conclusively shown by a simple control experiment. Figure 1D shows a TEM image recorded from a 2 ML LB film grown from gold particles complexed with HDA Langmuir monolayer, the reduction of the gold ions in this case having been accomplished by hydrazine reduction of the metal ions immediately after spreading of the Langmuir monolayer.<sup>16</sup> The gold nanoaggregate is extremely thick and of a dendritic morphology (Figure 1D). These gold structures did not show any preferred orientation (data not shown).

In conclusion, the large-scale synthesis of highly oriented, flat gold nanosheets and nanoribbons by the spontaneous reduction of aqueous chloroaurate ions by an HDA Langmuir monolayer has been shown. These anisotropic gold nanocrystals are expected to show interesting optical and electronic properties and are currently being investigated. Variation in the crystallography of the reducing Langmuir monolayer template may lead to control over face-specific nucleation of the gold nanocrystals and is an exciting possibility.

**Acknowledgment.** The authors thank Prof. C. N. R. Rao for illuminating discussions and use of HRTEM measurements at the JNCASR, Bangalore. Funding by the Department of Science and Technology, Government of India, is acknowledged.

**Supporting Information Available:** TEM images of the time-dependent growth of gold nanoribbons at the air-water interface (S1) and  $\pi$ - $A$  isotherms of HDA Langmuir monolayer on chloroauric acid solution with time (S2) (PDF). This material is available free of charge via the Internet at <http://pubs.acs.org>.

CM0256920